Nuclear magnetic resonance studies of hydrogen motion in nanostructured Laves-phase hydrides $ZrCr_2H_x$ and TaV_2H_x

2008 J. Phys.: Condens. Matter 20 275239

(http://iopscience.iop.org/0953-8984/20/27/275239)

IOP PUBLISHING JOURNAL OF PHYSICS: CONDENSED MATTER

J. Phys.: Condens. Matter **20** (2008) 275239 (8pp) doi:10.1088/0953-8984/20/27/275239

Nuclear magnetic resonance studies of hydrogen motion in nanostructured Laves-phase hydrides $ZrCr_2H_x$ and TaV_2H_x

A V Soloninin, A L Buzlukov, A V Skripov, B A Aleksashin, A P Tankeyev, A Ye Yermakov, N V Mushnikov, M A Uimin and V S Gaviko

Institute of Metal Physics, Urals Branch of the Academy of Sciences, Ekaterinburg 620041, Russia

Received 24 April 2008
Published 13 June 2008
Online at stacks.iop.org/JPhysCM/20/275239

Abstract

In order to study the mobility of hydrogen in nanostructured Laves-phase hydrides, we have measured the proton nuclear magnetic resonance (NMR) spectra and the proton spin–lattice and spin–spin relaxation rates in two nanostructured systems prepared by ball milling: $ZrCr_2H_3$ and $TaV_2H_{1+\delta}$. The proton NMR measurements have been performed at the resonance frequencies of 14, 23.8 and 90 MHz over the temperature ranges 11–424 K (for coarse-grained samples) and 11–384 K (for nanostructured samples). Hydrogen mobility in the ball-milled $ZrCr_2H_3$ is found to decrease strongly with increasing milling time. The experimental data suggest that this effect is related to the growth of the fraction of highly distorted intergrain regions where H mobility is much lower than in the crystalline grains. For the nanostructured $TaV_2H_{1+\delta}$ system, the ball milling is found to lead to a slight decrease in the long-range H mobility and to a suppression of the fast localized H motion in the crystalline grains.

1. Introduction

Nanostructured metal–hydrogen systems have become increasingly important both for applications and basic research. Because of a considerable volume fraction of grain boundary regions in nanostructured materials, their properties may strongly differ from those of the coarse-grained counterparts. One of the simplest methods of preparation of nanostructured hydrides is mechanical milling [1–3]. For a number of materials the milling leads to a significant acceleration of hydrogen absorption/desorption [4–6], which is of great importance for hydrogen-storage technologies. However, little is known about the mechanisms responsible for the changes in hydrogen reaction kinetics resulting from the milling. It is of special interest to elucidate the mechanism and the parameters of hydrogen diffusion in nanostructured hydrides. Nuclear magnetic resonance (NMR) measurements in metal–hydrogen systems can give microscopic information on the hydrogen mobility and hydrogen-induced changes in the electronic structure [7]. Previous applications of NMR to investigation of nanostructured hydrides include the studies of H motion in ball-milled vanadium–hydrogen [8] and graphite–hydrogen [9] systems, and the effects of paramagnetic centres resulting from the ball milling in magnesium–hydrogen systems with additives [10, 11].

In the present work, the proton NMR is applied to study the mobility of hydrogen in two nanostructured Laves-phase hydrides prepared by ball milling: $ZrCr_2H_x$ and TaV_2H_x. Hydrides of Laves-phase intermetallics are characterized by a rather high volumetric density of hydrogen and high hydrogen mobility [12]. The cubic (C15-type) Laves-phase system $ZrCr_2H_x$ shows (in the coarse-grained form) the highest H diffusivity [13] at $T < 200$ K among all the studied intermetallic hydrides. The coarse-grained C15-type system TaV_2H_x represents an example of a hydride with two well-separated scales of H jump motion [14, 15]. The faster jump process corresponds to localized H motion within the hexagons formed by tetrahedral interstitial g sites with Ta_2V_2 coordination, and the slower process is associated with H jumps from one g-site hexagon to another [15]. Because of

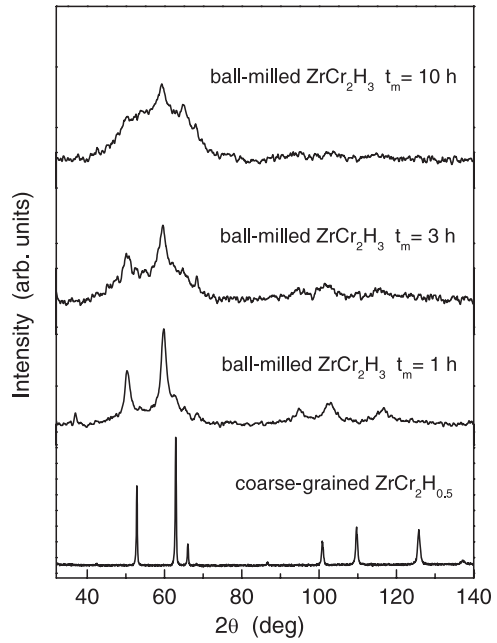

Figure 1. X-ray diffraction patterns (Cr Kα radiation) for the starting material $ZrCr_2H_{0.5}$ and nanostructured $ZrCr_2H_3$ systems prepared by ball milling for 1, 3 and 10 h.

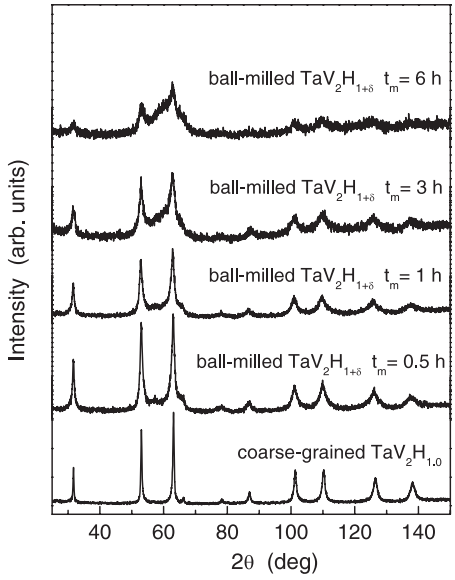

Figure 2. X-ray diffraction patterns (Cr Kα radiation) for the coarse-grained $TaV_2H_{1.0}$ and the nanostructured $TaV_2H_{1+\delta}$ systems prepared by ball milling for 0.5, 1, 3 and 6 h.

the high ratio of the hydrogen jump rates for the two processes (in the coarse-grained $TaV_2H_{1.1}$ this ratio at room temperature exceeds 10^3), it should be possible to study the effects of ball milling on each of the processes selectively. The aim of the present work is to investigate the changes in the parameters of H motion resulting from the milling of cubic Laves-phase hydrides. We have measured the proton NMR spectra and spin relaxation rates in ball-milled $ZrCr_2H_x$ and TaV_2H_x with different milling times over wide ranges of temperature and resonance frequency. Some preliminary results for $ZrCr_2H_x$ have been published in [11].

2. Experimental details

The starting materials for preparation of the nanostructured hydrides were powdered $ZrCr_2H_{0.5}$ and $TaV_2H_{1.0}$ with cubic C15-type structure and the lattice parameters $a = 7.278$ Å and 7.255 Å, respectively. These materials were placed together with brass balls (powder to ball mass ratio 1:140) into a brass vial. The vial was evacuated and subsequently filled with H_2 gas at a pressure of 110 kPa. The mechanical milling was performed at room temperature using a vibrating ball mill for periods t_m of 1, 3 and 10 h for $ZrCr_2H_x$, and 0.5, 1, 3 and 6 h for TaV_2H_x.

All the $ZrCr_2$-based samples rapidly absorbed hydrogen in the process of milling. For all the milling times studied, the hydrogen content estimated from the H_2 pressure change in the vial was approximately three H atoms per formula unit of $ZrCr_2$. The results of x-ray diffraction analysis for the $ZrCr_2$-based samples are shown in figure 1. The main crystalline phase of the ball-milled samples retains the C15-type structure with the lattice parameters $a = 7.608$ Å ($t_m = 1$ h), 7.645 Å (3 h) and 7.644 Å (10 h). These lattice parameters are close to those found for the coarse-grained $ZrCr_2H_x$ with $x \approx 3$ [16]. However, the diffraction peaks corresponding to the C15-type phase in the ball-milled samples are considerably broader than in the starting material. The average grain size estimated from the peak broadening in the sample with $t_m = 1$ h is 20 nm. The diffraction patterns for the ball-milled samples also contain traces of a C15-type phase with $a \approx 7.09$ Å and a very broad amorphous-like feature centred in the angle range of the most intense peaks of the C15-type phase. The intensity of this amorphous-like feature increases with increasing t_m; it becomes the dominant one in the diffraction pattern of the sample with $t_m = 10$ h. This feature can be attributed to highly distorted intergrain regions. In addition to the ball-milled $ZrCr_2H_3$ samples, we have prepared coarse-grained $ZrCr_2H_3$ by removing hydrogen from $ZrCr_2H_{0.5}$ at high-temperature (750 °C) and charging it again to the desired H content. The lattice parameter of the coarse-grained C15-type $ZrCr_2H_3$ is 7.599 Å.

The x-ray diffraction patterns of the TaV_2-based samples are shown in figure 2. In contrast to the $ZrCr_2$-based samples, the milling of $TaV_2H_{1.0}$ in a hydrogen atmosphere does not lead to an increase in the lattice parameter of the C15-type phase; the values of a for the ball-milled samples are nearly the same as in the coarse-grained $TaV_2H_{1.0}$. The average grain size estimated from the broadening of the peaks for the C15-type phase is 22 nm for $t_m = 0.5$ h, 15 nm for $t_m = 1$ h and 10–15 nm for $t_m = 3$ and 6 h. In addition to the C15-type phase, the ball-milled samples contain an unidentified phase giving the considerable contribution to the diffraction pattern between the most intense peaks of the C15-type phase (figure 2). This additional phase may contain hydrogen. In the following, the composition of the ball-milled TaV_2-based samples will be denoted as $TaV_2H_{1+\delta}$.

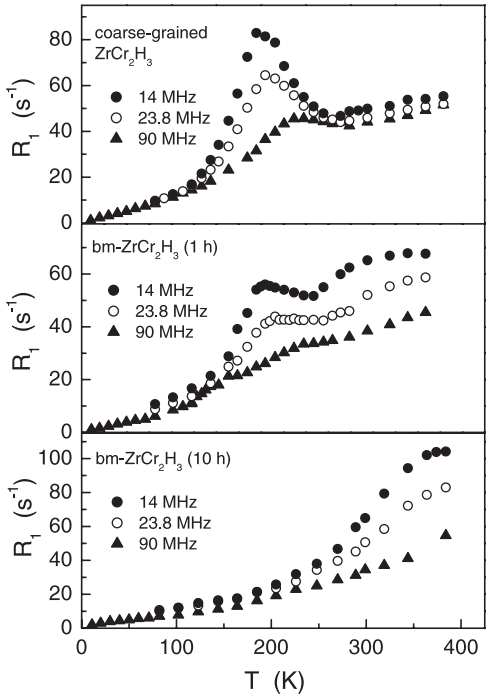

Figure 3. The temperature dependences of the proton spin–lattice relaxation rates measured at 14, 23.8 and 90 MHz for the coarse-grained $ZrCr_2H_3$ and for the nanostructured $ZrCr_2H_3$ systems prepared by ball milling for 1 and 10 h.

NMR measurements were performed on a modernized Bruker SXP pulse spectrometer at the frequencies $\omega/2\pi = 14$, 23.8 and 90 MHz. The proton NMR spectra were recorded by Fourier transforming the spin echo signals. The proton spin–lattice relaxation rates R_1 were measured using the saturation–recovery method. In all cases the recovery of the nuclear magnetization could be reasonably described by a single-exponential function. The proton spin–spin relaxation rates R_2 were measured using the two-pulse ($\pi/2$–τ–π) technique.

3. Results and discussion

3.1. Ball-milled $ZrCr_2H_3$

The temperature dependences of the proton spin–lattice relaxation rates measured at three resonance frequencies in the coarse-grained and two ball-milled ($t_m = 1$ and 10 h) samples of $ZrCr_2H_3$ are shown in figure 3. The R_1 results at $\omega/2\pi = 14$ MHz for all the samples studied are compared in figure 4. As can be seen from figures 3 and 4, the ball milling leads to dramatic changes in the behaviour of the spin–lattice relaxation rate. For the coarse-grained sample, the measured spin–lattice relaxation rate shows a frequency-dependent peak near 200 K. The position of this peak is consistent with the earlier results for polycrystalline $ZrCr_2H_x$ [17]. As the milling time increases, the amplitude of this peak rapidly decreases, and a new frequency-dependent peak starts to grow near 370 K. In order to avoid structural relaxation and recrystallization of the nanostructured samples, we have not performed any measurements for them above 384 K; therefore, only the low-temperature slope of the new peak is observed.

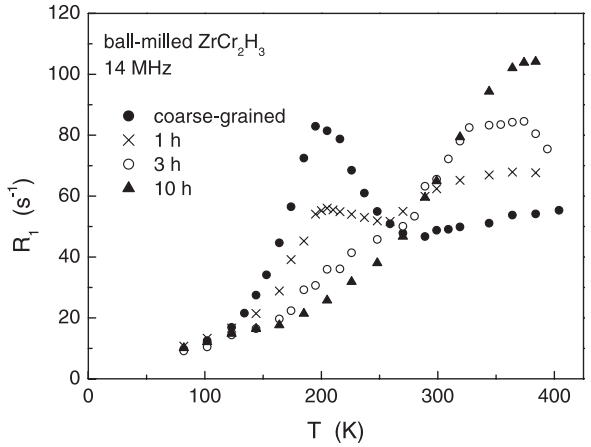

Figure 4. The temperature dependences of the proton spin–lattice relaxation rates measured at 14 MHz for the coarse-grained $ZrCr_2H_3$ and for the nanostructured $ZrCr_2H_3$ systems prepared by ball milling for 1, 3 and 10 h.

The measured proton spin–lattice relaxation rate R_1 in metal–hydrogen systems is usually determined by the sum of contributions resulting from the interactions of proton spins with conduction electrons (R_{1e}) and paramagnetic impurity ions (R_{1p}) and from the internuclear dipole–dipole interactions modulated by H motion (R_{1d}) [7],

$$R_1 = R_{1e} + R_{1p} + R_{1d}. \quad (1)$$

The frequency-independent electronic (Korringa) contribution is typically proportional to the temperature, $R_{1e} = C_eT$. For most metallic systems, the electronic contribution dominates at low temperatures, while the motional contribution becomes more important in the temperature range where the H jump rate τ_d^{-1} is between 10^7 and 10^{11} s^{-1}. The temperature dependence of R_{1d} shows a characteristic peak at the temperature at which $\omega\tau_d \approx 1$. In the limit of slow H diffusion ($\omega\tau_d \gg 1$), R_{1d} is proportional to $\omega^{-2}\tau_d^{-1}$, and in the limit of fast H diffusion ($\omega\tau_d \ll 1$), R_{1d} is proportional to τ_d being frequency-independent. The behaviour of the paramagnetic contribution R_{1p} is generally more complex; it depends on a number of parameters [18] including the spin–lattice relaxation time τ_i of paramagnetic ions.

The observed shift of the R_1 peak position from ~200 to 370 K as a result of ball milling indicates a strong decrease in the H jump rate. For the samples with intermediate milling times (1 and 3 h), both the low-temperature and high-temperature R_1 peaks appear to coexist. This suggests a coexistence of two H jump processes with different characteristic jump rates. It is natural to assume that the low-temperature R_1 peak originates from H motion in nearly undistorted crystalline grains of $ZrCr_2H_3$. The volume fraction of these grains is expected to decrease with increasing milling time. The high-temperature R_1 peak can be attributed to H motion in strongly distorted intergrain regions; the corresponding H jump rate at a given temperature is considerably lower than that in undistorted grains. For the sample milled for 10 h, no signs of the R_1 peak due to H motion

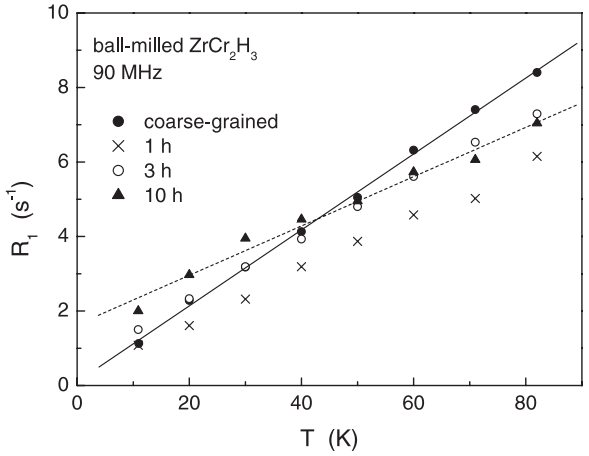

Figure 5. The low-temperature behaviour of the proton spin–lattice relaxation rates measured at 90 MHz. The solid and dashed lines show, respectively, the linear fits to the data for the coarse-grained $ZrCr_2H_3$ and for the nanostructured $ZrCr_2H_3$ system prepared by ball milling for 10 h.

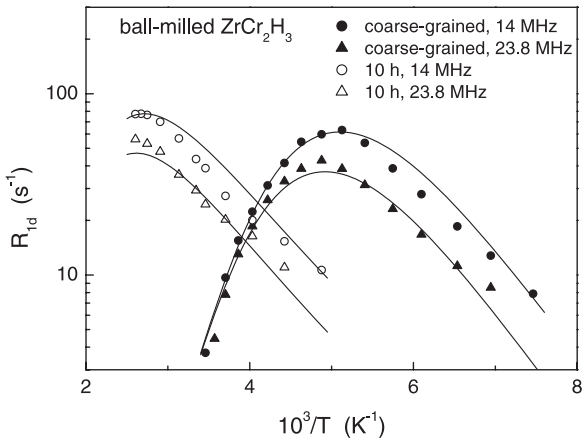

Figure 6. The dipolar contributions to the proton spin–lattice relaxation rate at 14 and 23.8 MHz as functions of the inverse temperature for the coarse-grained $ZrCr_2H_3$ and for the nanostructured $ZrCr_2H_3$ system prepared by ball milling for 10 h. The solid lines show the simultaneous fits of the BPP model with a Gaussian distribution of activation energies to the data.

in undistorted grains can be found. It should be noted that in the entire temperature range studied the spin–lattice relaxation is well described by a single-exponential function. The single-exponential behaviour of the spin–lattice relaxation in a system containing H atoms with different jump rates is expected to result from two mechanisms: the rapid exchange of H atoms between the grains and intergrain regions (above 200 K the corresponding exchange rate should be much higher than R_1) and the rapid equalization of spin polarization (*spin diffusion*) due to H–H dipole–dipole interaction.

In order to estimate the parameters of H jump motion, we have to determine the temperature dependence of the motional contribution R_{1d}, i.e., to subtract other contributions in equation (1) from the experimental results. Usually such a procedure is based on extrapolation of the low-temperature data. Figure 5 shows the temperature dependences of the proton spin–lattice relaxation rates measured at $\omega/2\pi = 90$ MHz in the low-temperature region ($T \leqslant 82$ K) where the hydrogen diffusion should be 'frozen out'. In this region, the temperature dependences of R_1 are well described by the expression $R_1 = C_eT + B$ for all the samples studied. The Korringa coefficient C_e is found to decrease with the milling time, from 0.102 s^{-1} K^{-1} for the coarse-grained sample to 0.066 s^{-1} K^{-1} for the sample milled for 10 h. Since C_e is proportional to the square of the density of electron states at the Fermi level, $N^2(E_F)$ [7], the observed changes in C_e suggest that the milling leads to the decrease in $N(E_F)$. The term B can be identified as the low-temperature limit of the paramagnetic contribution R_{1p} [7]. This term is found to increase with the milling time, from nearly zero for the coarse-grained sample to 1.6 s^{-1} for the sample milled for 10 h. For the coarse-grained $ZrCr_2H_3$, the proton spin–lattice relaxation rate at $T >$ 350 K should also be dominated by the electronic contribution. In fact, at $T > 350$ K the measured R_1 for this sample increases with increasing temperature (see figure 3), whereas the motional contribution R_{1d} is expected to decrease in this range. However, the values of R_1 at $T > 350$ K are somewhat higher than those obtained from the linear extrapolation of the low-temperature $R_{1e}(T)$ results. A similar feature has been reported for the coarse-grained $ZrCr_2H_x$ with low x [19] and for the isoelectronic system $HfCr_2H_x$ [20]. This feature may originate from nonlinear contributions to $R_{1e}(T)$ at high temperatures [21] or from a phase transition accompanied by a change in $N(E_F)$ at intermediate temperatures. In order to evaluate $R_{1d}(T)$ for the coarse-grained $ZrCr_2H_3$, we have approximated the behaviour of $R_{1e}(T)$ by two linear pieces: at $T < 200$ K, the linear extrapolation of the low-temperature C_eT term and at $T > 200$ K, the linear piece with a slightly higher slope ensuring that the values of R_{1e} above 350 K are nearly equal to the measured R_1.

Figure 6 shows the temperature dependences of the motional contribution $R_{1d} = R_1 - R_{1e}$ for the coarse-grained $ZrCr_2H_3$ at two resonance frequencies. In order to evaluate the parameters of H jump motion in the intergrain regions, we may use the R_1 data for the ball-milled sample with $t_m = 10$ h. The values of R_{1d} for this sample have been obtained by subtracting the linear extrapolation of the low-temperature $C_eT + B$ terms from the measured $R_1(T)$; the results at two resonance frequencies are included in figure 6. For both the coarse-grained $ZrCr_2H_3$ and the sample with $t_m = 10$ h, the observed frequency dependence of R_{1d} at the low-temperature slope of the $R_{1d}(T)$ peak is considerably weaker than the expected ω^{-2}. This feature, as well as the asymmetry of the $\lg R_{1d}$ versus T^{-1} plot can be accounted for in terms of the Bloembergen–Purcell–Pound (BPP) model with a Gaussian distribution of the activation energies E_a [22, 23]. In the framework of this model, the temperature dependence of R_{1d} is determined by the pre-exponential factor τ_{d0}^{-1} of the Arrhenius law for the H jump rate, the average activation energy $\overline{E_a}$ and the distribution width (dispersion) ΔE_a. We look for a set of parameters giving the best fit to the R_{1d} at two resonance frequencies *simultaneously*. The results of such simultaneous fits to the data are shown by full curves in figure 6. The parameters resulting from the fit for the coarse-grained $ZrCr_2H_3$ are

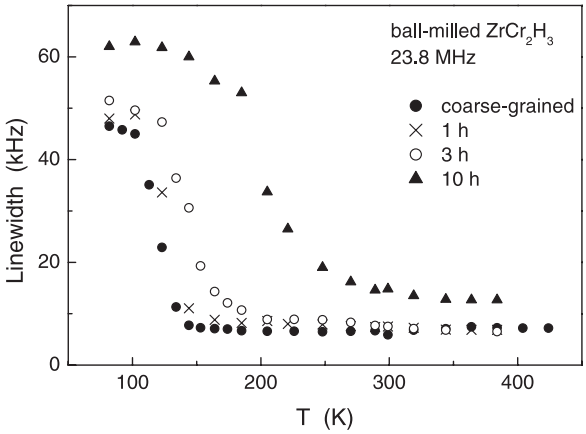

Figure 7. The temperature dependences of the width (full width at half-maximum) of the proton NMR spectra measured at 23.8 MHz for the coarse-grained $ZrCr_2H_3$ and for the nanostructured $ZrCr_2H_3$ systems prepared by ball milling for 1, 3 and 10 h.

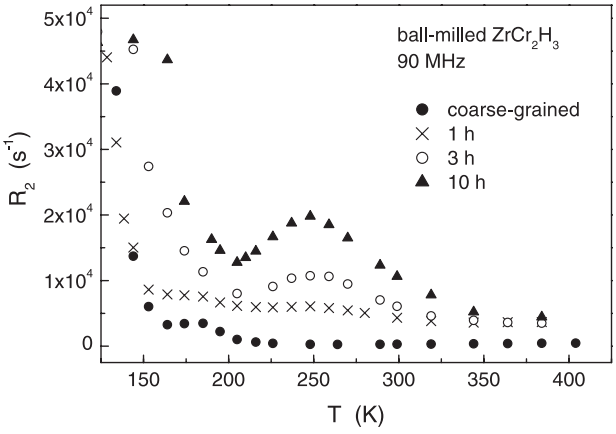

Figure 8. The temperature dependences of the proton spin–spin relaxation rates measured at 90 MHz for the coarse-grained $ZrCr_2H_3$ and for the nanostructured $ZrCr_2H_3$ systems prepared by ball milling for 1, 3 and 10 h.

$\tau_{d0}^{-1} = 1.9 \times 10^{14}$ s^{-1}, $\overline{E_a} = 246$ meV and $\Delta E_a = 34$ meV. For the ball-milled sample with $t_m = 10$ h, we assume that the value of τ_{d0}^{-1} is the same as for the coarse-grained sample and obtain $\overline{E_a} = 450$ meV and $\Delta E_a = 100$ meV. The quality of the fit for the ball-milled sample is poorer than for the coarse-grained one; this may be partially due to the fact that for the ball-milled sample we cannot observe the high-temperature slope of the R_1 peak and have a larger uncertainty in subtracting non-motional contributions to R_1.

Since we assume that the behaviour of R_1 in the ball-milled sample with $t_m = 10$ h is dominated by hydrogen in the highly distorted intergrain regions, our general conclusion is that the hydrogen mobility in intergrain regions is considerably lower than in the crystalline grains of $ZrCr_2H_3$. It is interesting to note that comparison of the NMR data in the crystalline C15-type hydrides $ZrV_2H_x(D_x)$ and in the amorphous hydrides of identical compositions [24] has also revealed a significant reduction of the hydrogen mobility in the amorphous samples. The opposite trend in the H mobility for most of the studied amorphous hydrides and their crystalline counterparts [25] is usually attributed to the fact that a structural disorder may give rise to the opening of new 'easy paths' for H diffusion. On the other hand, for Laves-phase hydrides the diffusion barriers are originally quite low, so that a structural disorder can only make the H diffusion more difficult. Similar arguments may be used for a qualitative interpretation of the decrease in H mobility resulting from ball milling of $ZrCr_2H_x$.

Figure 7 shows the temperature dependences of the ^{1}H NMR linewidth (full width at half-maximum) for the coarse-grained and ball-milled $ZrCr_2H_3$ samples. For all the samples studied, there is a range of sharp line narrowing. The narrowing becomes pronounced above the temperature at which the H jump rate exceeds the 'rigid-lattice' (low-temperature) linewidth [26]. Therefore, the observed shift of the T range of sharp line narrowing (figure 7) is consistent with the decrease in H mobility at long milling times. The value of the ^{1}H NMR linewidth at the high-temperature plateau is determined by a distribution of demagnetizing fields over the sample volume [26, 27]. As can be seen from figure 7, the width of such a distribution for the sample milled for 10 h is larger than for the other samples studied. This broadening may result from an increase in the number of paramagnetic centres appearing in the process of milling. Such a behaviour is consistent with the increase in the term B of the low-temperature spin–lattice relaxation rate at long milling times.

Figure 8 shows the temperature dependences of the proton spin–spin relaxation rates R_2 measured at 90 MHz. For all the samples studied, there is a range of sharp drop in R_2 with increasing temperature. This is the usual effect of motional averaging of the dipolar fields. The data shown in figure 8 suggest that the observed behaviour of R_2 is dominated by the contribution from protons in nearly undistorted grains. At higher temperatures, R_2 usually stops decreasing and becomes nearly constant. This change in behaviour is due to H diffusion through the magnetic field gradients inside each metallic particle [26]. As can be seen from figure 8, the behaviour of R_2 for the coarse-grained $ZrCr_2H_3$ is close to the expected one. However, for the ball-milled samples, an additional R_2 peak appears near 250 K, and its amplitude increases with increasing t_m. This feature cannot be explained in terms of internuclear dipole–dipole interactions modulated by H motion. The additional rate of dephasing of ^{1}H spins may arise if protons experience very slow fluctuations of the resonance frequency (or, equivalently, of the z-component of the local magnetic field). Such fluctuations are likely to appear for protons diffusing through a microscopically inhomogeneous medium.

It is interesting to note that the anomalous R_2 enhancement has been observed near the critical point of binary liquid mixtures showing a miscibility gap [28]. In the vicinity of the critical point, long-living microregions of different chemical composition are known to be formed. Molecular diffusion in such microscopically heterogeneous liquids leads to a time-dependent chemical shift experienced by a nucleus; this results in R_2 enhancement, as in the case of chemical exchange [28, 29]. The R_2 peak is expected to occur at the temperature for which the fluctuation rate becomes nearly

equal to the difference $\delta\omega$ between the resonance frequencies in different microregions [30]. For a diffusing particle, the mean displacement in a time t along any axis is $\sqrt{2Dt}$, where D is the diffusion coefficient. Therefore, the appropriate fluctuation rate can be roughly estimated as $D/2d^2$, where d is the average size of the microregions. In order to assess the length scale of d required to give rise to the R_2 peak near 250 K, we have to estimate the values of $\delta\omega$ and D (250 K). The value of $\delta\omega$ should be of the order of the maximum R_2 value [30], i.e. $\sim 10^4$ s^{-1}. For the coarse-grained $ZrCr_2H_{3.3}$, the value of D (250 K) measured by the pulsed-field-gradient NMR technique is 5.5×10^{-8} cm^2 s^{-1} [31]. Assuming that for the ball-milled $ZrCr_2H_3$ samples with $t_m = 3$ and 10 h, the H diffusivity at 250 K is about three times lower, i.e. $\sim 2 \times 10^{-8}$ cm^2 s^{-1}, we obtain $d \approx 100$ Å, or 10 nm. These rough estimates show that the spatial scale of inhomogeneity in our ball-milled $ZrCr_2H_3$ samples can lead to a peak of the proton spin–spin relaxation rate. Thus, the proton spin–spin relaxation rate can, in principle, be used as a probe of the inhomogeneity of nanostructured hydrides.

The proton R_2 peak near 230 K was also reported for *coarse-grained* $ZrCr_2H_x$ with low x ($x = 0.2$, 0.3 and 0.5) [32]. As compared to the concentrated hydride $ZrCr_2H_3$, these low-x compounds have considerably higher H mobilities [17, 19] and much lower values of the magnetic susceptibility and the proton Knight shift [17, 33]. The R_2 peak in the low-x $ZrCr_2H_x$ was also interpreted in terms of H diffusion through a microscopically inhomogeneous medium; however, the inhomogeneity was assumed to be *intrinsic* (clusters of H atoms or long-period spin-density waves) [32]. It should be noted that the maximum R_2 values for the peak observed in the low-$x$$ZrCr_2H_x$ did not exceed 5×10^2 s^{-1} [32], being lower than even the background R_2 values for the ball-milled $ZrCr_2H_3$ (see figure 8). This means that the amplitude of the resonance frequency fluctuations for the ball-milled $ZrCr_2H_3$ should be much higher than in the case of low-$x$$ZrCr_2H_x$. It is probable that paramagnetic centres appearing in the process of milling [11] can contribute to the R_2 enhancement.

3.2. Ball-milled $TaV_2H_{1+\delta}$

The temperature dependences of the proton spin–lattice relaxation rates measured at $\omega/2\pi = 23.8$ and 90 MHz for the coarse-grained $TaV_2H_{1.0}$ and the ball-milled $TaV_2H_{1+\delta}$ ($t_m = 0.5$ and 6 h) are shown in figure 9. As can be seen from this figure, for the coarse-grained $TaV_2H_{1.0}$ the temperature dependence of R_1 exhibits two peaks. Such a behaviour reflects the coexistence of two well-separated frequency scales of H jump motion [14, 15]. The fast localized motion within g-site hexagons [15] is responsible for the low-temperature R_1 peak observed near 120 K, and the slower jump process leading to long-range H diffusion gives rise to the high-temperature R_1 peak near 300 K. The amplitude of the low-temperature peak is smaller than that of the high-temperature one; this can be explained by the combined effect of two factors. First, in contrast to long-range diffusion, a localized motion averages out only a part of the 'rigid-lattice' dipole–dipole interaction.

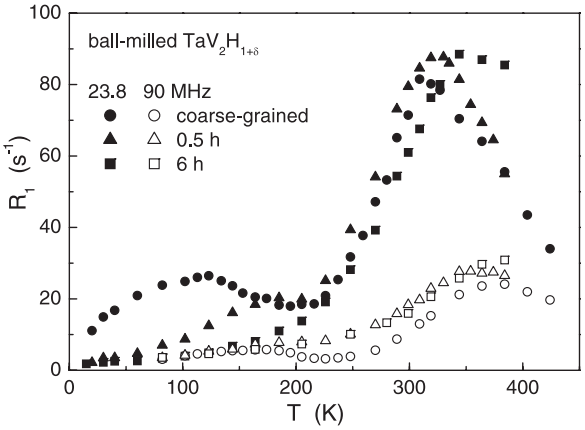

Figure 9. The temperature dependences of the proton spin–lattice relaxation rates measured at 23.8 and 90 MHz for the coarse-grained $TaV_2H_{1.0}$ and for the nanostructured $TaV_2H_{1+\delta}$ systems prepared by ball milling for 0.5 and 6 h.

Second, only a fraction of all H atoms is known to participate in the fast localized motion in TaV_2H_x [15]. As can be seen from figure 9, the milling leads to a rapid smearing out of the low-temperature R_1 peak. This suggests that the localized H motion in TaV_2H_x is very sensitive to distortions of the g-site hexagons. Even slight distortions of the hexagons are expected to result in very broad distributions of the H jump rates within the hexagons. These observations support the idea that the hydrogen jump rates strongly depend on the corresponding intersite distances [34].

The amplitude of the high-temperature R_1 peak remains nearly unchanged, and its position shifts to higher T with the increasing milling time (figure 9). For the ball-milled $TaV_2H_{1+\delta}$ samples, this peak can still be attributed to H diffusion in slightly distorted C15-type grains, and its shift suggests a certain decrease in H mobility with increasing t_m. In contrast to the case of the ball-milled $ZrCr_2H_3$, in the studied temperature range we have not found any R_1 features that could be ascribed to H motion in strongly distorted intergrain regions of the ball-milled $TaV_2H_{1+\delta}$. The most probable reason for this is that H atoms (if any) in the intergrain regions of the ball-milled $TaV_2H_{1+\delta}$ have a very low mobility, so they cannot give rise to any R_1 peak below 390 K.

Because of the presence of the fast localized H motion, the electronic contribution to the proton spin–lattice relaxation rate in TaV_2H_x is difficult to estimate. For the coarse-grained $TaV_2H_{1.0}$, we adopt the estimate $C_e = 3.8 \times 10^{-3}$ s^{-1} K^{-1} from [14] and assume that this value remains unchanged in the ball-milled $TaV_2H_{1+\delta}$. In any case, in the region of the high-temperature R_1 peak the electronic contribution R_{1e} is much lower than the dipolar contribution R_{1d}. Figure 10 shows the behaviour of R_{1d} at 23.8 MHz in the region of the high-temperature peak for the coarse-grained $TaV_2H_{1.0}$ and the ball-milled $TaV_2H_{1+\delta}$ ($t_m = 3$ and 6 h). In order to evaluate the parameters of the long-range H diffusion, we have used the BPP model with a Gaussian distribution of activation energies. The results of the fits of this model to the R_{1d} data are shown by full curves in figure 10. For the coarse-grained $TaV_2H_{1.0}$, the corresponding

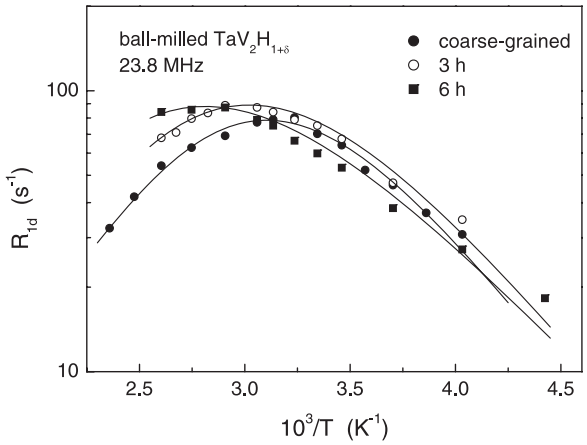

Figure 10. The dipolar contributions to the proton spin–lattice relaxation rate at 23.8 MHz as functions of the inverse temperature for the coarse-grained $TaV_2H_{1.0}$ and for the nanostructured $TaV_2H_{1+\delta}$ systems prepared by ball milling for 3 and 6 h.

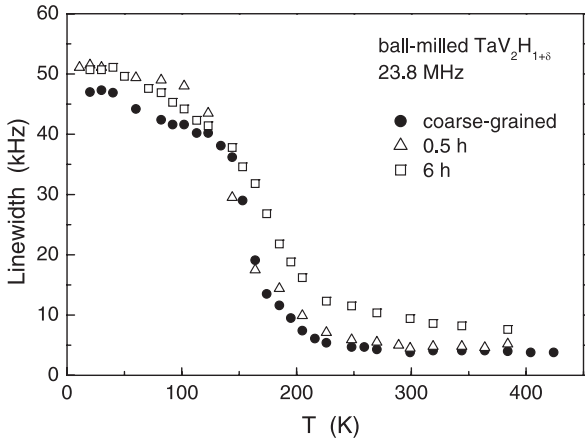

Figure 11. The temperature dependences of the width (full width at half-maximum) of the proton NMR spectra measured at 23.8 MHz for the coarse-grained $TaV_2H_{1.0}$ and for the nanostructured $TaV_2H_{1+\delta}$ systems prepared by ball milling for 0.5 and 6 h.

fit parameters are $\overline{E_a}$ = 198 meV, ΔE_a = 16 meV, and $\tau_{d0} = 4.8 \times 10^{-12}$ s. The values of $\overline{E_a}$ and τ_{d0} for the coarse-grained $TaV_2H_{1.0}$ are close to those derived previously [14] from the proton spin–lattice relaxation data for $TaV_2H_{0.87}$. For the ball-milled samples, we assume that the value of τ_{d0} is the same as for the coarse-grained $TaV_2H_{1.0}$, and obtain $\overline{E_a}$ = 203 meV, ΔE_a = 22 meV for t_m = 3 h and $\overline{E_a}$ = 216 meV, ΔE_a = 31 meV for t_m = 6 h. Thus, the milling leads to the increase in both the average activation energy and the width of the activation energy distribution.

Figure 11 shows the temperature dependences of the ^{1}H NMR linewidth (full width at half-maximum) for the coarse-grained $TaV_2H_{1.0}$ and ball-milled $TaV_2H_{1+\delta}$ (t_m = 0.5 and 6 h). Besides the usual range of sharp motional narrowing (∼150–170 K), the temperature dependence of the proton linewidth for the coarse-grained $TaV_2H_{1.0}$ exhibits an additional step-like feature near 50 K. This feature indicates that a certain part of the 'rigid-lattice' dipole–dipole interaction is averaged out by the fast localized H motion in $TaV_2H_{1.0}$. For the ball-milled samples, no such well-pronounced feature is observed. As the milling time increases, the range of substantial line narrowing shifts to higher temperatures (figure 11); this is consistent with a certain decrease in long-range H mobility at long t_m. As can be seen from figure 11, the milling also leads to the increase in the linewidth at the high-temperature plateau. This is likely to originate from the growth of the number of paramagnetic centres appearing in the process of milling. In contrast to the case of $ZrCr_2H_3$, the proton spin–spin relaxation rate R_2 in the ball-milled $TaV_2H_{1+\delta}$ (not shown) does not exhibit any anomalous behaviour in the range of the high-temperature plateau. One of the possible reasons for this is the strong difference between the long-range H diffusivities [31] in the crystalline grains of $ZrCr_2H_3$ and $TaV_2H_{1.0}$. Thus, the observability of the R_2 peak in nanostructured hydrides is likely to depend on a certain combination of the experimental parameters (D, $\delta\omega$, d). A search for other nanostructured hydrides showing the R_2 enhancement is in progress.

4. Conclusions

The results of our proton NMR measurements for the ball-milled Laves-phase hydrides $ZrCr_2H_3$ indicate that the hydrogen mobility in this system strongly decreases with increasing milling time. The experimental data suggest that this effect is related to the growth of the fraction of highly distorted intergrain regions where H mobility is much lower than in the crystalline grains. These results are consistent with the previous data [24] for amorphous counterparts of Laves-phase hydrides. The anomalous peak of the proton spin–spin relaxation rate has been revealed for the ball-milled $ZrCr_2H_3$ near 250 K. Such a peak may originate from slow fluctuations of the resonance frequency of a proton diffusing through a spatially inhomogeneous medium on the length scale of about 10 nm.

In contrast to the case of the ball-milled $ZrCr_2H_3$, in the studied temperature range 11–384 K our proton NMR data for the ball-milled $TaV_2H_{1+\delta}$ do not show any features that could be ascribed to H motion in strongly distorted intergrain regions. Therefore, all the results for this system should be attributed to slightly distorted C15-type grains. It is found that the ball milling leads to a suppression of the fast localized H motion over g-site hexagons, which suggests that this motion is extremely sensitive to distortions of the hexagons. The ball milling also results in a certain decrease in the long-range H mobility in C15-type grains of $TaV_2H_{1+\delta}$.

Acknowledgments

This work was supported by the Russian Foundation for Basic Research (Grant No. 06-02-16246), the Priority Programme 'Basic Energy Problems' of the Russian Academy of Sciences and the Russian Science Support Foundation.

References

[1] Orimo S, Fujii H and Ikeda K 1996 *Acta Mater.* **45** 331
[2] Konstanchuk I G, Ivanov E Y and Boldyrev V V 1998 *Russ. Chem. Rev.* **67** 69

[3] Huot J, Tremblay M L and Schulz R 2003 *J. Alloys Compounds* **356/357** 603
[4] Chen Y and Williams J S 1995 *J. Alloys Compounds* **217** 181
[5] Zaluska A, Zaluski L and Ström-Olsen J O 1999 *J. Alloys Compounds* **288** 217
[6] Barkhordarian G, Klassen T and Bormann R 2004 *J. Alloys Compounds* **364** 242
[7] Barnes R G 1997 *Hydrogen in Metals III* ed H Wipf (Berlin: Springer) p 93
[8] Orimo S, Kimmerle F and Majer G 2001 *Phys. Rev.* B **63** 094307
[9] Majer G, Stanik E and Orimo S 2003 *J. Alloys Compounds* **356/357** 617
[10] Yermakov A Ye, Mushnikov N V, Uimin M A, Gaviko V S, Tankeyev A P, Skripov A V, Soloninin A V and Buzlukov A L 2006 *J. Alloys Compounds* **425** 367
[11] Skripov A V, Soloninin A V, Buzlukov A L, Tankeyev A P, Yermakov A Ye, Mushnikov N V, Uimin M A and Gaviko V S 2007 *J. Alloys Compounds* **446/447** 489
[12] Skripov A V 2003 *Defect Diffus. Forum* **224/225** 75
[13] Renz W, Majer G, Skripov A V and Seeger A 1994 *J. Phys.: Condens. Matter* **6** 6367
[14] Skripov A V, Rychkova S V, Belyaev M Yu and Stepanov A P 1990 *J. Phys.: Condens. Matter* **2** 7195
[15] Skripov A V, Cook J C, Sibirtsev D S, Karmonik C and Hempelmann R 1998 *J. Phys.: Condens. Matter* **10** 1787
[16] Fruchart D, Rouault A, Shoemaker C B and Shoemaker D P 1980 *J. Less-Common Met.* **73** 363
[17] Skripov A V, Belyaev M Yu and Stepanov A P 1991 *Solid State Commun.* **78** 909
[18] Phua T T, Beaudry B J, Peterson D T, Torgeson D R, Barnes R G, Belhoul M, Styles G A and Seymour E F W 1983 *Phys. Rev.* B **28** 6227
[19] Skripov A V and Belyaev M Yu 1993 *J. Phys.: Condens. Matter* **5** 4767
[20] Skripov A V, Soloninin A V, Buzlukov A L, Voyevodina L S, Cook J C, Udovic T J and Hempelmann R 2005 *J. Phys.: Condens. Matter* **17** 5011
[21] Göring R, Lukas R and Bohmhammel K 1981 *J. Phys. C: Solid State Phys.* **14** 5675
[22] Shinar J, Davidov D and Shaltiel D 1984 *Phys. Rev.* B **30** 6331
[23] Markert J T, Cotts E J and Cotts R M 1988 *Phys. Rev.* B **37** 6446
[24] Rychkova S V, Belyaev M Yu, Skripov A V and Stepanov A P 1988 *Sov. Phys.—Solid State* **30** 1285
[25] Richter D, Hempelmann R and Bowman R C 1992 *Hydrogen in Intermetallic Compounds II* ed L Schlapbach (Berlin: Springer) p 97
[26] Cotts R M 1978 *Hydrogen in Metals I* ed G Alefeld and J Völkl (Berlin: Springer) p 227
[27] Drain L E 1962 *Proc. Phys. Soc.* **80** 1380
[28] Anderson J E 1969 *J. Chem. Phys.* **50** 1474
[29] Anderson J E and Liu K J 1968 *J. Chem. Phys.* **49** 2850
[30] Witteveen J 1997 *Phys. Rev.* B **55** 8083
[31] Majer G, Renz W, Seeger A, Barnes R G, Shinar J and Skripov A V 1995 *J. Alloys Compounds* **231** 220
[32] Stoddard R D, Balbach J J, Conradi M S and Skripov A V 1999 *Phys. Rev.* B **59** 3769
[33] Galoshina E V, Kozhanov V N and Skripov A V 2002 *Phys. Met. Metallogr.* **93** 48
[34] Skripov A V 2005 *J. Alloys Compounds* **404–406** 224